

Chapter 3

Homogeneous atmosphere above a ground surface

3.1 Introduction

In the previous chapter we have seen that a point source generates spherical waves in an unbounded homogeneous atmosphere. We showed that the sound pressure level at a receiver in the spherical sound field can be calculated from the sound power level of the source, taking into account the geometrical attenuation due to spherical spreading and the attenuation due to atmospheric absorption.

In practice the source or the receiver, or both, are often close to a ground surface. In this case the calculation of the sound pressure level at the receiver is more complex, as will be described in this chapter. The ground surface reflects sound waves, so there are not only direct sound waves from the source to the receiver but also reflected sound waves. The interference between direct waves and reflected waves has a considerable effect on the sound field (see Fig. 3.1). In Chaps. 4 and 5 we will see that the interference is affected by atmospheric gradients and atmospheric turbulence. For small distances between the source and the receiver, however, these atmospheric effects can be neglected.

For an acoustically hard ground surface, *e.g.* concrete, the calculation of the sound pressure level is relatively simple. For an acoustically absorbing ground surface, *e.g.* grassland, the calculation is more complex.

3.2 Reflection of spherical waves by a ground surface

We consider the geometry shown in Fig. 3.2, with a harmonic monopole source and a receiver in a homogeneous atmosphere above a ground surface. We use an rz coordinate system in the vertical plane through the source and the receiver;

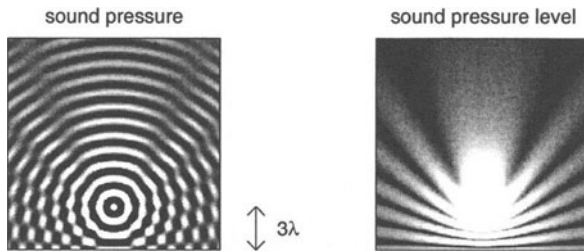


Figure 3.1. Fields of the sound pressure (left) and the sound pressure level (right), generated by a harmonic monopole source at a height of three wavelengths (3λ) above an acoustically hard ground surface, in a homogeneous atmosphere. Regions of low amplitude corresponding to destructive interference are clearly visible as dark regions in the field of the sound pressure level, but are also visible in the field of the sound pressure. The fields have been calculated with Eq. (3.2), using $Q = 1$ for a hard ground surface.

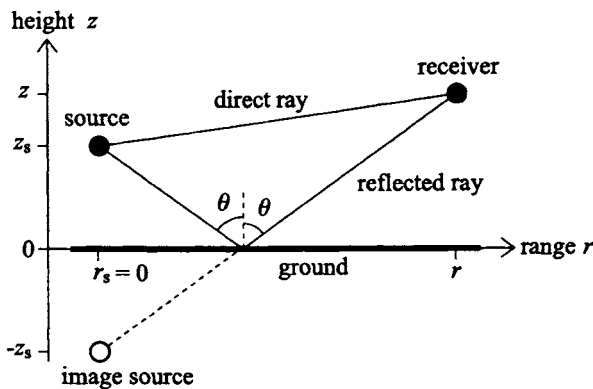


Figure 3.2. Geometry with a source and a receiver above a ground surface. Also indicated is the image source below the ground surface.

r is the horizontal range measured from the source and z is the height above the ground surface. The source is at position $(r_s = 0, z_s)$ and the receiver is at position (r, z) .

The source is characterized by the *free field*, i.e. the sound field of the source in an unbounded homogeneous atmosphere. The complex pressure amplitude of the free field is (see Sec. 2.4)

$$p_{\text{free}} = S \frac{\exp(ikR_1)}{R_1}, \quad (3.1)$$

where S is a constant, k is the wave number, and R_1 is the distance from the source.

The complex pressure amplitude at the receiver in the geometry shown in Fig. 3.2 can be written as (see Sec. D.4)

$$p_c = S \frac{\exp(ikR_1)}{R_1} + QS \frac{\exp(ikR_2)}{R_2}, \quad (3.2)$$

with $R_1 = \sqrt{r^2 + (z - z_s)^2}$ and $R_2 = \sqrt{r^2 + (z + z_s)^2}$. The quantity Q in this equation is called the spherical-wave reflection coefficient; this quantity can be calculated with Eq. (D.54), Eq. (D.58), or Eq. (D.72) in Appendix D. The value of Q is a complex number, in general. Equation (3.2) can be interpreted in terms of two sound rays: the direct ray and the ray reflected by the ground surface (see Fig. 3.2). The path length of the direct ray is R_1 and the path length of the reflected ray is R_2 . Equation (3.2) can also be interpreted in terms of two sources: the real source above the ground surface and the image source below the ground surface (see Fig. 3.2). The distance between the receiver and the real source is R_1 and the distance between the receiver and the image source is R_2 .

Atmospheric absorption is taken into account in Eqs. (3.1) and (3.2) by including a small imaginary term in the wave number (see Sec. 2.5).

The complex pressure amplitude given by Eq. (3.2) is unaffected if the positions of the source and the receiver are interchanged. This is called the principle of reciprocity [121, 106], which holds also in an inhomogeneous atmosphere without wind (and even in an inhomogeneous atmosphere with wind if the wind direction is reversed).

3.3 Spherical-wave reflection coefficient and ground impedance

The spherical-wave reflection coefficient Q in Eq. (3.2) is a function of the following four quantities (see Sec. D.4):

- wave number k (or frequency $f = kc/2\pi$),
- distance R_2 ,

- reflection angle θ (see Fig. 3.2),
- normalized ground impedance Z .

The normalized ground impedance Z is a quantity that characterizes the ground surface acoustically (see Appendix C). The value of Z is a complex number, which depends on the frequency of the sound waves and on the structure of the ground. Various models exist for the calculation of the normalized ground impedance from parameters that characterize the structure of the ground. The most important parameter is the flow resistivity, denoted by the symbol σ .

To define the flow resistivity, we consider a situation in which a pressure difference over a slab of porous material forces air to flow through the slab. The flow resistivity is equal to the ratio of the pressure difference to the flow velocity, divided by the thickness of the slab. This is analogous to the definition of electric resistance. We express flow resistivity in units of $\text{kPa}\cdot\text{s}\cdot\text{m}^{-2}$.

The concept of flow resistivity is also used for natural grounds such as grassland. Thus, grassland is modeled as a porous medium. A typical value of the flow resistivity for grassland is $\sigma = 200 \text{ kPa}\cdot\text{s}\cdot\text{m}^{-2}$. The flow resistivity of a material can be measured directly, but is often determined indirectly from acoustic measurements [6, 8, 31, 32, 37, 15, 48, 50, 96, 127, 87]. In the latter case the flow resistivity is treated as an adjustable parameter, and is called the *effective* flow resistivity. Values of the effective flow resistivity of natural absorbing grounds, such as grassland, forest floors, and sandy grounds, range roughly from $\sigma = 10 \text{ kPa}\cdot\text{s}\cdot\text{m}^{-2}$ to $\sigma = 1000 \text{ kPa}\cdot\text{s}\cdot\text{m}^{-2}$.

Delany and Bazley [39] developed an empirical model for the calculation of the impedance of fibrous absorbing materials. This model works well also for natural grounds such as grassland. Zwicker and Kosten [161] and Attenborough [4, 5, 6, 7, 10, 11] developed theoretical models for the calculation of the impedance. In the theoretical models, the ground is approximated as a semi-infinite porous medium, or as a porous layer with a rigid backing. In the numerical examples in this book, we model absorbing ground as a semi-infinite porous medium; unless indicated otherwise, we use the four-parameter model developed by Attenborough [5] for the calculation of the impedance; the parameters of the model are specified in Sec. C.4.

To gain insight into the ground reflection of spherical waves, we note that at high frequency the spherical-wave reflection coefficient Q is approximately equal to the plane-wave reflection coefficient R_p , which is given by (see Sec. D.2)

$$R_p = \frac{Z \cos \theta - 1}{Z \cos \theta + 1}. \quad (3.3)$$

For an acoustically hard ground surface we have $Z = \infty$ (and $\sigma = \infty$) so we find $R_p = 1$. In this case we also have $Q = 1$ (see Sec. D.4). An acoustically hard surface is usually referred to as a rigid surface. Examples are a concrete surface and a water surface.

An acoustically absorbing ground surface has a finite impedance. Let us consider a situation in which the ground surface has a finite impedance and

both the source height and the receiver height are very small compared with the horizontal distance between the source and the receiver. In this case the reflection angle θ approaches $\pi/2$ (see Fig. 3.3). The limit $\theta \rightarrow \pi/2$ is called the limit of grazing incidence. It follows from Eq. (3.3) that R_p approaches -1 in the limit of grazing incidence. Hence, the spherical-wave reflection coefficient at high frequency also approaches -1 in the limit of grazing incidence. The path lengths of the direct ray and the reflected ray are approximately equal in this case ($R_1 \approx R_2$), so the two terms on the right-hand side of Eq. (3.2) have approximately equal magnitudes but opposite signs. This corresponds to a destructive interference between direct sound waves and sound waves reflected by the ground surface. Thus, the sound pressure above a finite-impedance ground surface is very low in the limit of grazing incidence.

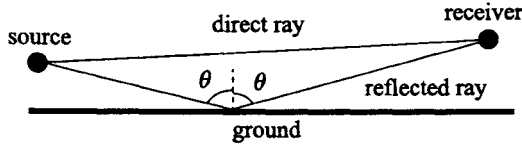


Figure 3.3. The reflection angle θ approaches $\pi/2$ in the limit of grazing incidence.

3.4 Relative sound pressure level

From Eqs. (3.1) and (3.2) we have

$$p_c = p_{\text{free}} \left[1 + Q \frac{R_1}{R_2} \exp(ikR_2 - ikR_1) \right]. \quad (3.4)$$

This relation between p_c and p_{free} can also be expressed in terms of the corresponding sound pressure levels L_p and $L_{p,\text{free}}$, respectively. From Eq. (2.8) we have $L_p = 10 \lg(\frac{1}{2}|p_c|^2/p_{\text{ref}}^2)$ and $L_{p,\text{free}} = 10 \lg(\frac{1}{2}|p_{\text{free}}|^2/p_{\text{ref}}^2)$. This gives

$$L_p = L_{p,\text{free}} + \Delta L, \quad (3.5)$$

with

$$\Delta L = 10 \lg \left(\frac{|p_c|^2}{|p_{\text{free}}|^2} \right). \quad (3.6)$$

The quantity ΔL will be referred to as the *relative sound pressure level*, and plays an important role in this book. From Eqs. (3.4) and (3.6) we find

$$\Delta L = 10 \lg \left| 1 + Q \frac{R_1}{R_2} \exp(ikR_2 - ikR_1) \right|^2. \quad (3.7)$$

The relative sound pressure level ΔL represents the deviation from the free field sound pressure level due to the presence of the ground surface. Both positive and negative values of ΔL occur.

Negative values of ΔL occur in the case of destructive interference between direct sound waves and reflected sound waves. Complete destructive interference ($\Delta L = -\infty$) occurs if the second term in the argument of the logarithmic function in Eq. (3.7) is equal to -1.

Positive values of ΔL occur in the case of constructive interference between direct and reflected sound waves. For a rigid ground we have $Q = 1$ and the maximum value of ΔL is $10 \lg 2^2 \approx 6$ dB, as follows from Eq. (3.7) for $R_1 \approx R_2$. For absorbing ground we often have $|Q| < 1$, so the maximum value of ΔL is lower than 6 dB. In some situations, however, we have $|Q| > 1$ and values of ΔL higher than 6 dB occur; this can be attributed to the so-called surface wave [108, 51, 146] (see also Sec. H.5), which is contained implicitly in the expressions for the spherical-wave reflection coefficient Q given in Sec. D.4.

As noted before, atmospheric absorption is taken into account by including a small imaginary term in the wave number (see Sec. 2.5). In many practical situations, however, we have $R_1 \approx R_2$, and atmospheric absorption can be neglected in Eq. (3.7). Only in situations with a high source and a high receiver, the distances R_1 and R_2 may be considerably different, and atmospheric absorption should be taken into account in Eq. (3.7).

Substitution of Eq. (2.9) for $L_{p,\text{free}}$ into Eq. (3.5) gives

$$L_p = L_W - 10 \lg 4\pi R_1^2 - \alpha R_1 + \Delta L. \quad (3.8)$$

This equation, with relative sound pressure level ΔL defined by Eq. (3.6), is not restricted to the geometry shown in Fig. 3.2. Any deviation from the free field of a source can be represented by ΔL defined by Eq. (3.6). If the deviation is due to a ground reflection in a homogeneous atmosphere, ΔL is given by Eq. (3.7). The deviation may also be due to other effects. In Chaps. 4 to 7 we will use the relative sound pressure level to represent deviations due to atmospheric refraction, atmospheric turbulence, irregular terrain, and noise barriers.

Instead of the relative sound pressure level ΔL , the equivalent quantity ‘excess attenuation’ is also used in atmospheric acoustics. The excess attenuation is equal to $-\Delta L$.

The quantities L_p , L_W , α , and ΔL in Eq. (3.8) are functions of frequency, in general. The function $L_W(f)$, for example, is the narrow band spectrum of the sound power level of the source (see Sec. 2.6). The function $\Delta L(f)$ is the corresponding spectrum of the relative sound pressure level. The spectrum $\Delta L(f)$ should not be considered as a narrow band spectrum, as the value of $\Delta L(f)$ does not depend on a narrow band width [whereas the values of $L_p(f)$ and $L_W(f)$ do depend on the narrow band width]. The term ‘continuous’ spectrum is more appropriate for the spectrum $\Delta L(f)$.

The narrow band or continuous spectra in Eq. (3.8) can be converted to octave band spectra or 1/3-octave band spectra. Logarithmic summation of

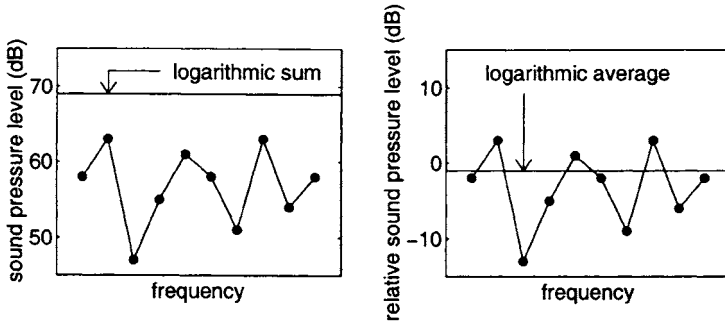


Figure 3.4. Example of logarithmic summation of the sound pressure level (left) and logarithmic averaging of the relative sound pressure level (right). The summation and averaging may be over the frequencies in an octave band or a 1/3-octave band.

Eq. (3.8) over a 1/3-octave or octave band yields the approximate relation

$$L_p(f_c) = L_W(f_c) - 10 \lg 4\pi R_1^2 - \alpha(f_c)R_1 + \Delta L(f_c). \quad (3.9)$$

The quantities $L_p(f_c)$, $L_W(f_c)$, and $\alpha(f_c)R_1$ in this relation have been defined in Sec. 2.6 and the quantity $\Delta L(f_c)$ is equal to the ‘logarithmic average’ $10 \lg (\frac{1}{N} \sum' 10^{\Delta L(f)/10})$, where the sum is over N frequencies in the band; we assume that the frequencies are equidistant on a linear scale (see Fig. 2.5 and Sec. B.4). To derive Eq. (3.9) from the narrow band relation (3.8) one neglects the variation of $L_W(f)$ and $-\alpha(f)R_1$ over the band. This variation can usually not be neglected, but Eq. (3.9) is still used as an approximation (see Sec. 2.6). Figure 3.4 shows an example of logarithmic summation of the sound pressure level and logarithmic averaging of the relative sound pressure level. The logarithmic average is dominated by the highest levels.

3.5 Examples

In this section we present graphs of the relative sound pressure level, calculated with Eq. (3.7) for the geometry shown in Fig. 3.2. We use the rz coordinate system shown in Fig. 3.2 to denote the positions of the source and the receiver. We use the following notation above the graphs:

- source ($r_s = 0, z_s$), where z_s is expressed in meters,
- receiver (r, z), where r and z are expressed in meters,
- frequency f in Hz,
- flow resistivity σ of the ground surface in $\text{kPa}\cdot\text{s}\cdot\text{m}^{-2}$.

Figure 3.5 shows the field of the relative sound pressure level ΔL for a harmonic monopole source of 500 Hz at a height of 2 m above a rigid ground surface ($\sigma = \infty$). The field contains distinct regions where the level ΔL is low (lower than the lower limit of -20 dB of the grey level scale). These regions correspond to destructive interference between direct sound waves and sound waves reflected by the ground surface. For a rigid ground surface we have $Q = 1$, and it follows from Eq. (3.7) that the minima of the relative sound pressure level occur for $\exp(ikR_2 - ikR_1) = -1$, or $k(R_2 - R_1) = (2n+1)\pi$, with $n = 0, 1, 2, \dots$. Using $k = 2\pi f/c$, we find that the minima occur for

$$R_2 - R_1 = (n + \frac{1}{2})\lambda, \quad (3.10)$$

where $\lambda = c/f$ is the wavelength. Thus, destructive interference occurs if the path length difference $R_2 - R_1$ between the direct sound ray and the reflected sound ray is equal to $(n + \frac{1}{2})\lambda$, so that direct waves and reflected waves have a phase difference of 180° . With increasing height in Fig. 3.5, one successively passes the regions corresponding to $n = 0, 1, 2, \dots$.

Figure 3.6 demonstrates the effect of 1/3-octave band averaging, both for a rigid ground surface and for an absorbing ground surface. For the rigid ground surface, deep interference minima occur in the continuous spectrum $\Delta L(f)$, while the minima in the 1/3-octave band spectrum are considerably less deep (cf. Fig. 3.4). For the absorbing ground surface, the interference minima in the continuous spectrum are considerably less pronounced than for the rigid ground surface, and consequently the effect of 1/3-octave band averaging on the minima is smaller than for the rigid ground surface.

For the rigid ground surface, the relative sound pressure level in Fig. 3.6 approaches 6 dB below a frequency of about 100 Hz (see Sec. 3.4). For the absorbing ground surface, the relative sound pressure level in Fig. 3.6 approaches 6 dB at very low frequencies, below about 16 Hz (at very low frequency the reflection coefficient Q approaches unity and the absorbing ground surface can be considered as a rigid ground surface); at frequencies around 100 Hz the relative sound pressure level is considerably lower for the absorbing ground surface than for the rigid ground surface. With increasing frequency in the graphs in Fig. 3.6, one successively passes the interference minima corresponding to $n = 0, 1, 2, \dots$ (see above).

In Fig. 3.6, and in many practical situations, we have $z \ll r$ and $z_s \ll r$. In this case the frequencies of the interference minima can be calculated with Eqs. (3.11) and (3.12) below. Equation (3.11) is valid for a rigid ground surface and Eq. (3.12) is valid for an absorbing ground surface.

For a rigid ground surface we have from Eq. (3.10) the relation $R_2 - R_1 = (n + \frac{1}{2})\lambda$ at the interference minima, with $n = 0, 1, 2, \dots$. From $z \ll r$ and $z_s \ll r$ we find $R_2 - R_1 \approx 2zz_s/r$. Using $\lambda = c/f$, we find that the interference minima for a rigid ground surface occur at the frequencies

$$f_n = (n + \frac{1}{2}) \frac{rc}{2zz_s}. \quad (3.11)$$

Substitution of the values $z_s = 2$ m, $z = 2$ m, and $r = 30$ m, which were used for Fig. 3.6, gives the relation $f_n = (2n + 1)f_0$ with $f_0 = 637.5$ Hz. The interference minima in Fig. 3.6 for the rigid ground surface occur at frequencies that agree with this relation.

For the absorbing ground surface, the interference minima occur at slightly lower frequencies. This is due to the fact that the reflection by a finite-impedance ground surface causes a phase change of a sound wave. The spherical-wave reflection coefficient Q in Eq. (3.7) is a complex number, and can be written as $Q = |Q| \exp(i\vartheta)$, where $|Q|$ is the absolute value and ϑ is the argument. For an absorbing ground surface, it follows from Eq. (3.7) that the minima of the level ΔL occur for $\exp(ikR_2 - ikR_1 + i\vartheta) = -1$, or $k(R_2 - R_1) + \vartheta = (2n + 1)\pi$, with $n = 0, 1, 2, \dots$. Using $R_2 - R_1 \approx 2zz_s/r$, we find that the interference minima for an absorbing ground surface occur at the frequencies

$$f_n = \left(n + \frac{1}{2} - \frac{\vartheta}{2\pi}\right) \frac{rc}{2zz_s}. \quad (3.12)$$

The argument ϑ is a positive quantity; this can be seen from Eq. (3.3), using $Q \approx R_p$ and the fact that the imaginary part of the normalized impedance Z is positive (see Sec. C.4). Consequently, the interference minima for an absorbing ground surface occur at lower frequencies than for a rigid ground surface.

The interference minima in Fig. 3.6 are deeper for the rigid ground surface than for the absorbing ground surface. This can be explained as follows. For the rigid ground surface, direct waves and reflected waves have approximately equal amplitudes, so the waves cancel each other almost completely in regions where the phases are opposite. For the absorbing ground surface, the amplitude of reflected waves is smaller than the amplitude of direct waves, due to the absorption of acoustic energy by the ground, so only a partial cancellation occurs. This can also be seen from Eq. (3.7). For the rigid ground surface we have $Q = 1$, and the second term in the argument of the logarithm is approximately equal to -1 at the interference minima (using $R_1 \approx R_2$). For the absorbing ground surface we have $|Q| < 1$ at the interference minima, and the term is smaller (less negative) than -1.

Figure 3.7 illustrates the effect of the choice of the impedance model (see Sec. 3.3) on the spectrum of the relative sound pressure level. The model developed by Delany and Bazley [39] yields a slightly different spectrum than the model developed by Attenborough [5] does.

Figures 3.8 and 3.9 illustrate the effect of receiver range r (*i.e.* the horizontal distance between the source and the receiver) on the spectrum of the relative sound pressure level, for a rigid ground surface and an absorbing ground surface, respectively. For the rigid ground surface, the interference minima shift to higher frequency with increasing range r , in agreement with Eq. (3.11). For the absorbing ground surface, the first interference minimum becomes broader and deeper with increasing range r . This is a consequence of the destructive interference between direct sound waves and reflected sound waves, which occurs for grazing incidence on a finite-impedance ground surface (see Sec. 3.3).

Figures 3.10 and 3.11 illustrate the effect of receiver height z on the spectrum of the relative sound pressure level, for a rigid ground surface and an absorbing ground surface, respectively. For the rigid ground surface, the interference minima shift to lower frequency with increasing height z , in agreement with Eq. (3.11). For the absorbing ground surface, the first interference minimum becomes broader and deeper with decreasing height z . Again, this is a consequence of the destructive interference for grazing incidence on a finite-impedance ground surface.

Figure 3.12 illustrates the effect of flow resistivity σ of the ground surface on the spectrum of the relative sound pressure level. With increasing σ , the first interference minimum shifts to higher frequency.

Figure 3.13 illustrates the effect of finite dimensions of a sound source on the spectrum of the relative sound pressure level. For this figure we use a rectangular xyz coordinate system, where x and y are horizontal coordinates and z is the height above the ground surface. Source positions are denoted as $(x_s = 0, y_s, z_s)$ and the receiver position is $(x = 100, y = 0, z = 2)$, where coordinates are expressed in meters. The figure shows three spectra:

- a spectrum for a point source at position $(0,0,2)$,
- a spectrum for a set of 256 incoherent point sources distributed uniformly over a square of 4 m^2 in the yz plane, with $-1 \leq y_s \leq 1$ and $1 \leq z_s \leq 3$,
- a spectrum for a set of 100 incoherent point sources distributed uniformly over a line segment with a length of 200 m, located above the y axis, with $x_s = 0$, $-100 \leq y_s \leq 100$, and $z_s = 2$.

By ‘incoherent point sources’ we mean that the contributions of the point sources to the received sound pressure level are summed logarithmically (see Sec. 2.6), corresponding to logarithmic averaging of ΔL . This approach is reasonable if the point sources have no phase relations with each other, or if the phase differences between the sources show random fluctuations. The set of point sources distributed uniformly over the line segment, for example, can be used to calculate the average noise from cars on a road, as the cars have no phase relations with each other. A continuous distribution of point sources over a line is called an incoherent line source [75]. The representation of a car by a point source is studied in Refs. [59, 60].

The differences between the three spectra shown in Fig. 3.13 are small. The second interference minimum in the spectrum for the single point source is absent in the spectrum for the set of point sources distributed over the square. In other situations, however, the effect of finite dimensions of a sound source may be larger.

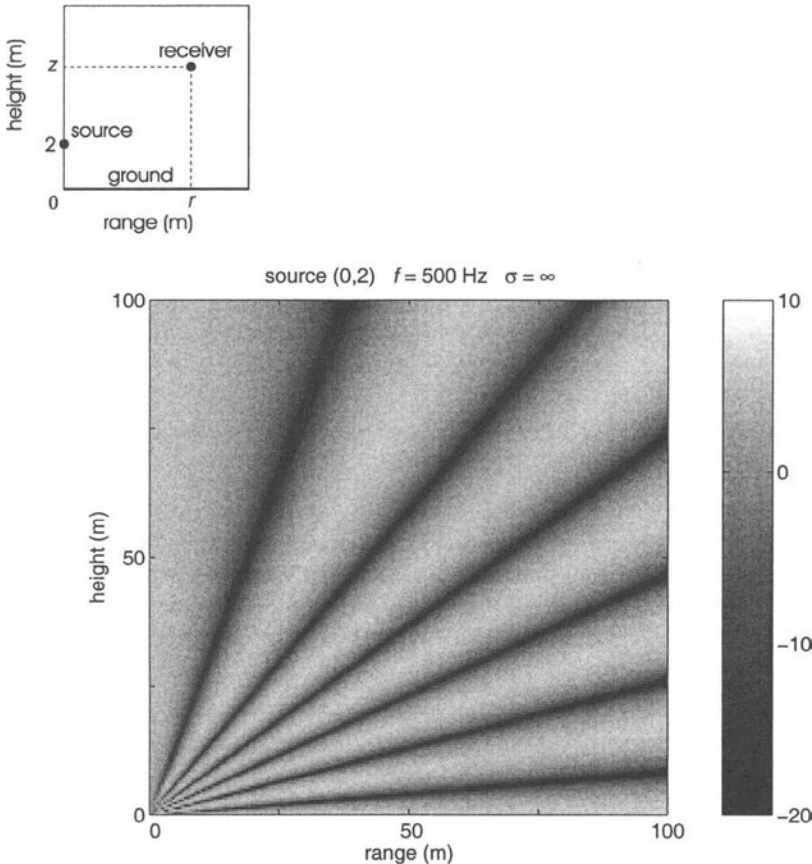


Figure 3.5. Field of relative sound pressure level ΔL as a function of receiver range r and receiver height z . The grey level represents the value of ΔL in dB, as indicated by the vertical bar. The geometry is shown above the graph. The source is a harmonic source with a frequency of 500 Hz. The source is located at range $r = 0$ and height $z = 2$ m. The ground surface is rigid ($\sigma = \infty$) and the atmosphere is homogeneous. The notation above the graph is explained in Sec. 3.5.

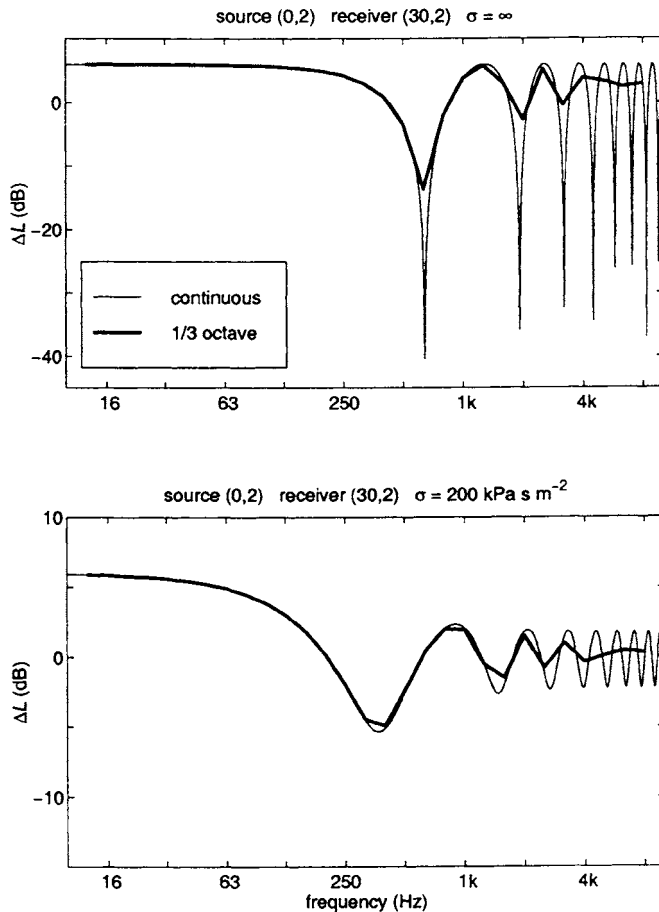


Figure 3.6. Continuous spectrum and one-third-octave band spectrum of the relative sound pressure level, for a rigid ground surface (upper graph) and an absorbing ground surface (lower graph). The impedance of the absorbing ground surface was calculated with a model developed by Attenborough [5], using a flow resistivity of $200 \text{ kPa}\cdot\text{s}\cdot\text{m}^{-2}$.

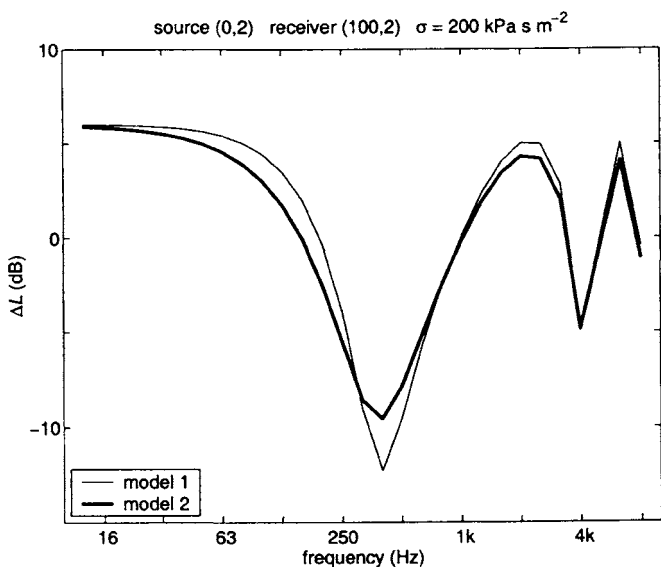


Figure 3.7. One-third-octave band spectrum of the relative sound pressure level, for an absorbing ground surface with a flow resistivity of $200 \text{ kPa}\cdot\text{s}\cdot\text{m}^{-2}$. The ground impedance was calculated from the flow resistivity with a model developed by Delany and Bazley [39] ('model 1') and a model developed by Attengborough [5] ('model 2').

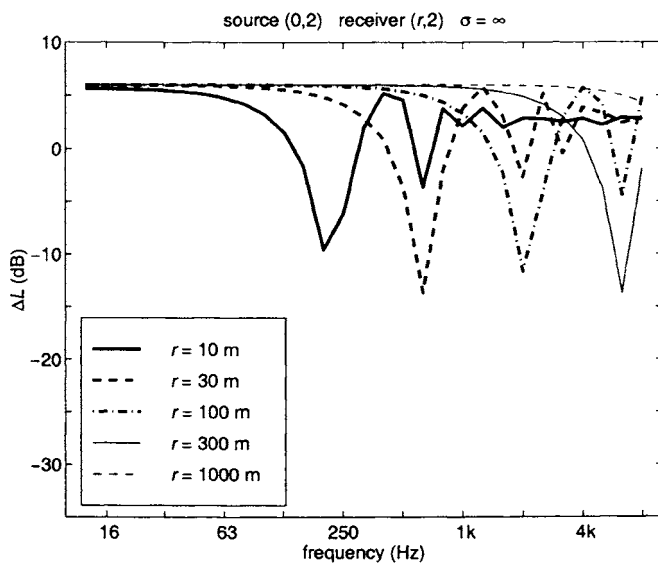


Figure 3.8. One-third-octave band spectrum of the relative sound pressure level, for five receiver ranges r (see legend) and a rigid ground surface.

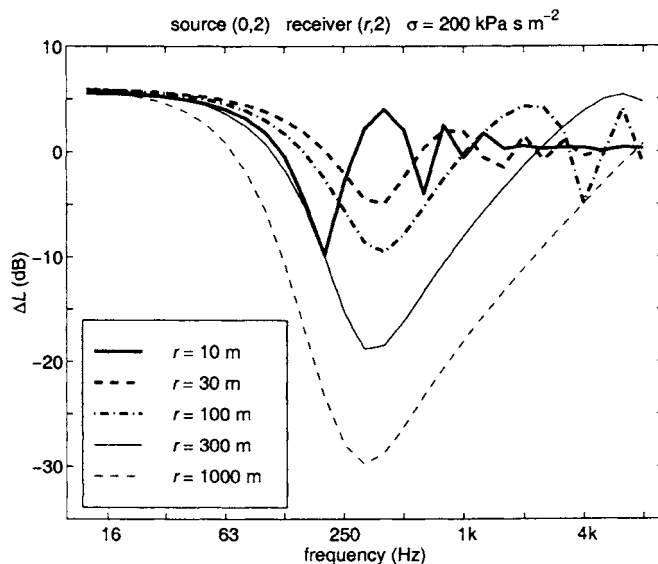


Figure 3.9. As Fig. 3.8, for an absorbing ground surface.

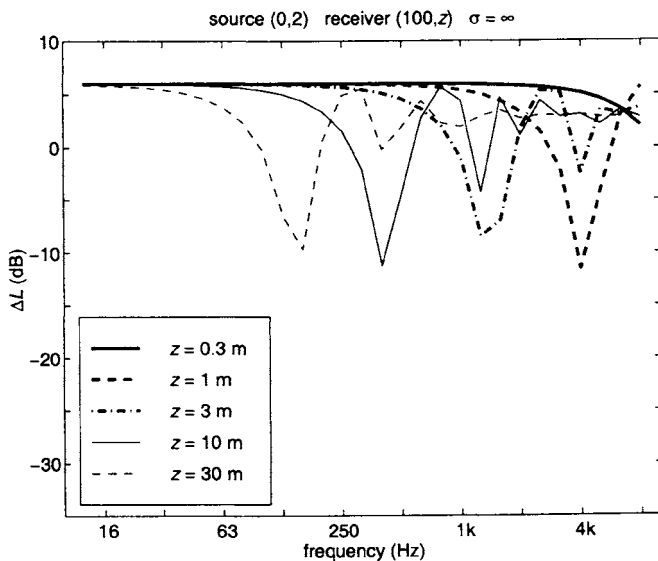


Figure 3.10. One-third-octave band spectrum of the relative sound pressure level, for five receiver heights z (see legend) and a rigid ground surface.

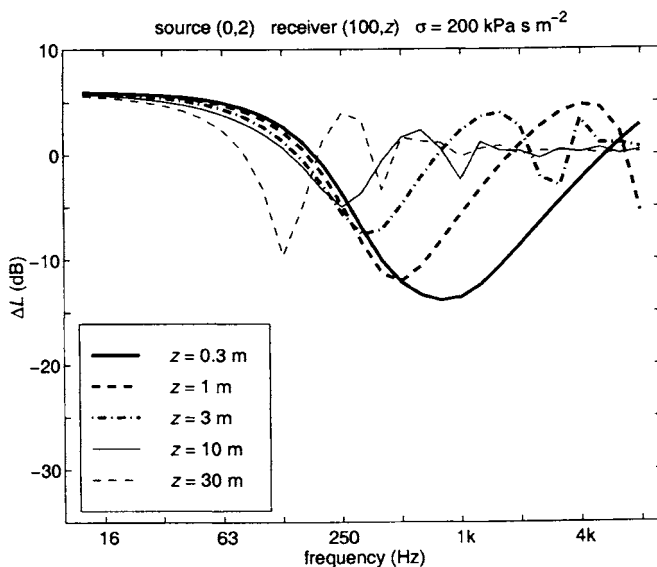


Figure 3.11. As Fig. 3.10, for an absorbing ground surface.

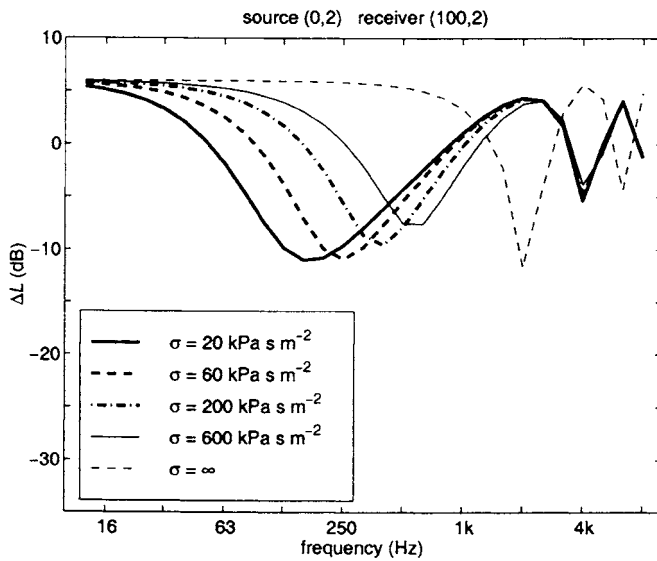


Figure 3.12. One-third-octave band spectrum of the relative sound pressure level, for five values of the flow resistivity σ of the ground surface (see legend).

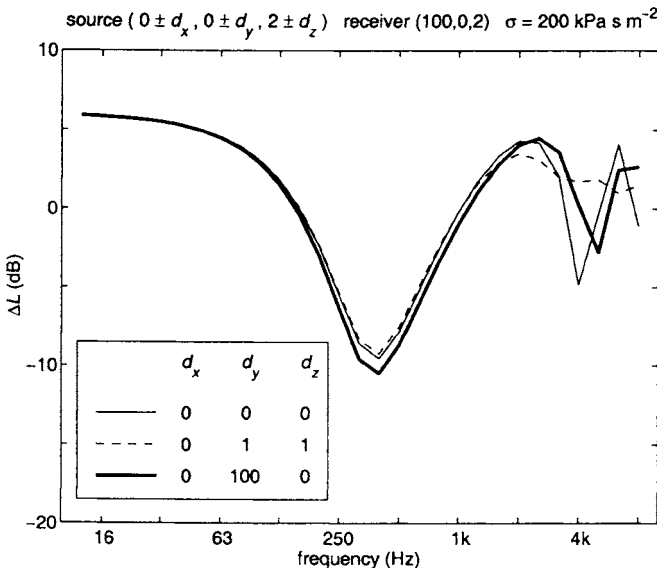


Figure 3.13. Example of the effect of finite dimensions of a source on the 1/3-octave band spectrum of the relative sound pressure level (see the text).

Chapter 4

Atmospheric refraction

4.1 Introduction

In the previous chapter we studied sound propagation in a non-refracting atmosphere over a ground surface. In general, the assumption of a non-refracting atmosphere is justified only for small propagation distances. For propagation distances of the order of 100 m or more, atmospheric refraction often has large effects on received sound pressure levels, in particular if the source and the receiver are close to the ground, at heights of a few meters or less.

In this chapter we study sound propagation in a refracting atmosphere over a ground surface. In Sec. 4.2 we describe the physical process of atmospheric refraction, which is caused predominantly by vertical gradients of the temperature and the wind speed. Empirical relations for the vertical profiles of the temperature and the wind speed in the atmospheric surface layer are given in Appendix N. In Sec. 4.3 we introduce the profile of the effective sound speed, which depends on the profiles of the temperature and the wind speed.

In Sec. 4.4 we describe the ray model for sound propagation in a refracting atmosphere. The ray model is useful for a qualitative understanding of atmospheric sound propagation. It is less useful for accurate computations of sound pressure levels, in particular in situations with irregular sound speed profiles, owing to complex effects such as the focusing of sound rays at so-called caustic points. A ray model for smooth sound speed profiles is described in Appendix L.

In Sec. 4.5 we describe three accurate numerical methods for sound propagation in a refracting atmosphere over a ground surface:

- the Fast Field Program (FFP),
- the Crank-Nicholson Parabolic Equation (CNPE) method,
- the Green's Function Parabolic Equation (GFPE) method.

The three methods are described in detail in Appendices F, G, and H, respectively.

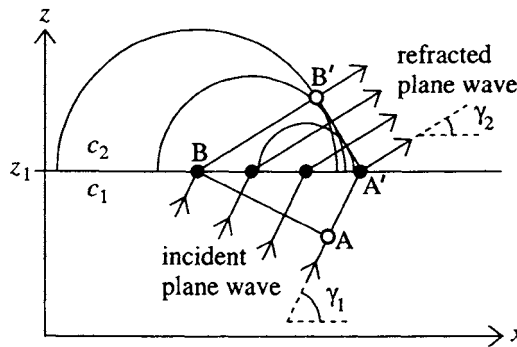


Figure 4.1. Refraction of a plane wave in an atmosphere with sound speed c_1 for $z \leq z_1$ and sound speed c_2 for $z > z_1$. Line segment AB is a wave front of the incident wave. Secondary sources (solid circles) at the interface $z = z_1$ generate spherical waves which form wave front A'B' of the refracted wave.

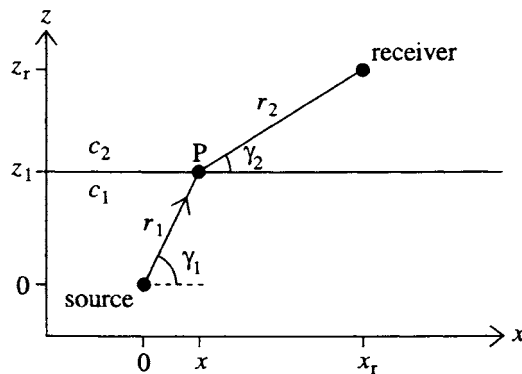


Figure 4.2. Refracted sound ray from a point source to a receiver, in the same atmosphere as in Fig. 4.1. The origin of the xz coordinate system is chosen at the position of the source. Point P is at position (x, z_1) and the receiver is at position (x_r, z_r) .

In Sec. 4.6 we present numerical examples. The examples illustrate the accuracy of the computational methods in various situations.

4.2 Atmospheric refraction

Atmospheric refraction was described in Sec. 2.2 as a change of the propagation direction of a sound wave due to a sound speed gradient in the atmosphere. The propagation direction at a point was defined as the direction of the vector normal to the wave front through the point. The wave fronts of a plane wave in a non-refracting atmosphere are plane surfaces; in this case the propagation direction is independent of position. Refraction of a plane wave is illustrated in Fig. 4.1, for an atmosphere in which the sound speed c is a simple function of height z :

$$c(z) = \begin{cases} c_1 & \text{for } z \leq z_1 \\ c_2 & \text{for } z > z_1, \end{cases} \quad (4.1)$$

where c_1 and c_2 are constants and z_1 is the height indicated in Fig. 4.1. In general, the function $c(z)$ is called the (vertical) *sound speed profile*. The figure shows a plane wave in the region $z < z_1$ incident on the interface at height z_1 . The elevation angle of a plane wave is defined as the angle between the propagation direction and the (horizontal) x axis; the elevation angle of the incident plane wave is γ_1 . All points of the interface at height z_1 can be considered as secondary point sources (this is Huygen's principle [106]). Spherical waves generated by the secondary sources form a plane wave in the region $z > z_1$, with elevation angle γ_2 .

We consider line segment AB of the wave front at time t , which has moved to A'B' at time $t + \delta t$. The time interval δt is equal to $|AA'|/c_1$, and also equal to $|BB'|/c_2$, where $|AA'|$ and $|BB'|$ are the lengths of line segments AA' and BB', respectively. From $|AA'| = |A'B| \cos \gamma_1$ and $|BB'| = |A'B| \cos \gamma_2$, where $|A'B|$ is the length of line segment A'B, we find

$$\frac{\cos \gamma_1}{c_1} = \frac{\cos \gamma_2}{c_2}. \quad (4.2)$$

This is Snell's law of refraction (see also Sec. D.3). For an atmosphere with a continuous sound speed profile $c(z)$, instead of the discontinuous profile given by Eq. (4.1), Snell's law states that the elevation angle γ of a plane wave varies with z in such a way that the ratio $\cos \gamma(z)/c(z)$ is constant.

In Fig. 4.1 we have $\gamma_2 < \gamma_1$, corresponding to $c_2 > c_1$; the atmosphere is called a downward refracting atmosphere in this case. In the opposite case with $\gamma_2 > \gamma_1$ and $c_2 < c_1$, the atmosphere is called an upward refracting atmosphere.

The wave fronts of a point source in a non-refracting atmosphere are spheres. In a refracting atmosphere, the spheres are deformed by the effect of refraction. A curved wave front can be approximated locally by a plane wave front. The propagation of such a plane wave front obeys Snell's law of refraction. An

equivalent statement is that the curved sound rays from a point source, *i.e.* the curves perpendicular to the wave fronts of the point source, obey Snell's law for sound rays:

$$\frac{\cos \gamma(z)}{c(z)} = \text{constant along a sound ray}, \quad (4.3)$$

where $\gamma(z) = \arctan(dz/dx)$ is the elevation angle of the sound ray at height z . This is illustrated in Fig. 4.2 for an atmosphere with the sound speed profile given by Eq. (4.1). The sound ray consists of two straight segments, with a discontinuous slope at $z = z_1$. In an atmosphere with a continuous sound speed profile $c(z)$, instead of the discontinuous profile given by Eq. (4.1), the sound rays are curves with a continuous slope.

The travel time of a sound wave along the path represented by a sound ray is always smaller than the travel time along a slightly deformed path. In other words, a sound wave follows the path between the source and the receiver that corresponds to a (local) minimum of the travel time. This is Fermat's principle of minimum travel time (a more general statement is that a sound wave follows the path that corresponds to a stationary travel time; see Ref. [106]).

To illustrate Fermat's principle we consider a deformation of the path shown in Fig. 4.2 by varying the x coordinate of point P. The travel time t is given by $t = r_1/c_1 + r_2/c_2$, with $r_1 = \sqrt{x^2 + z_1^2}$ and $r_2 = \sqrt{(x_r - x)^2 + (z_r - z_1)^2}$. The derivative of the travel time with respect to the x coordinate of point P is $\partial t/\partial x = (x/r_1)/c_1 - [(x_r - x)/r_2]/c_2$, or $\partial t/\partial x = \cos \gamma_1/c_1 - \cos \gamma_2/c_2$. From Fermat's principle we have $\partial t/\partial x = 0$, which gives $\cos \gamma_1/c_1 = \cos \gamma_2/c_2$, *i.e.* Snell's law.

4.3 Effective sound speed

In a non-moving atmosphere, *i.e.* an atmosphere without wind, sound waves travel with the adiabatic sound speed, which is a function of the temperature of the atmosphere (see Secs. 2.2 and A.2). An atmosphere with wind is called a moving atmosphere. The computation of sound propagation in a moving atmosphere is more complex than the computation of sound propagation in a non-moving atmosphere. Fortunately, a moving atmosphere can be approximated by a non-moving atmosphere with an *effective sound speed* $c_{\text{eff}} = c + u$, where c is the adiabatic sound speed and u is the (horizontal) component of the wind velocity in the direction of sound propagation. The idea behind this approximation is that a sound wave travels faster if the atmosphere moves in the propagation direction ($u > 0$) and slower if the atmosphere moves in the opposite direction ($u < 0$) [40]. A more rigorous justification of the effective sound speed approximation is given in Sec. E.3. In general, the effective sound speed approximation is valid in situations in which sound waves travel with relatively small elevation angles, such as situations with the source and the receiver near the ground. For large elevation angles, the effective sound speed approximation

is not valid. The effective sound speed c_{eff} will often be referred to simply as the sound speed c .

Spatial variations of the temperature and the wind velocity in the atmosphere correspond to spatial variations of the effective sound speed. These variations cause atmospheric refraction. In situations with a flat, homogeneous ground surface, it is usually a good approximation to assume that the temperature, the wind velocity, and the effective sound speed are functions of height z only:

$$c_{\text{eff}}(z) = c(z) + u(z). \quad (4.4)$$

The atmosphere is called a layered atmosphere or a stratified atmosphere in this case. The function $c_{\text{eff}}(z)$ is called the (effective) sound speed profile.

Empirical expressions for the vertical profiles of the temperature and the wind speed are given in Appendix N. These profiles should be considered as average profiles, averaged over a period of typically ten minutes (variations of the profiles on smaller time scales are considered in Chap. 5). The expressions given in Appendix N are valid for the atmospheric surface layer, which has a height of typically 100 m. The profiles are characterized by large vertical gradients near the ground surface. At the ground surface, the wind speed is approximately zero, due to friction at the ground surface. With increasing height, the wind speed increases while the vertical derivative of the wind speed decreases. The variation of the wind speed is largest in the first few meters above the ground surface. The shape of the wind speed profile depends on the roughness of the ground surface. Air flowing over a ground surface is ‘slowed down’ more effectively by a rough surface, *e.g.* grassland, than by a smooth surface, *e.g.* a water surface.

The shape of the temperature profile is similar to the shape of the wind speed profile. The variation of the temperature is largest near the ground surface and decreases with increasing height. In the daytime, the temperature usually decreases with increasing height. At night, the temperature usually increases with increasing height.

A realistic profile of the effective sound speed in the atmospheric surface layer is the logarithmic profile

$$c_{\text{eff}}(z) = c_0 + b \ln \left(\frac{z}{z_0} + 1 \right) \quad (4.5)$$

with parameters c_0 , b , and z_0 . Parameter c_0 is the sound speed at the ground surface; the precise value of c_0 is unimportant, and we use $c_0 = 340$ m/s. Parameter z_0 is called the (aerodynamic) roughness length of the ground surface; typical values are between 0.01 m and 0.1 m for grassland and between 10^{-4} m and 10^{-3} m for a water surface. We use $z_0 = 0.1$ m, unless indicated otherwise. Typical values of parameter b in Eq. (4.5) are 1 m/s for a downward refracting atmosphere and -1 m/s for an upward refracting atmosphere. Figure 4.3 shows the logarithmic profile (4.5) for $c_0 = 340$ m/s, $z_0 = 0.1$ m, and $b = 1$ m/s. For an

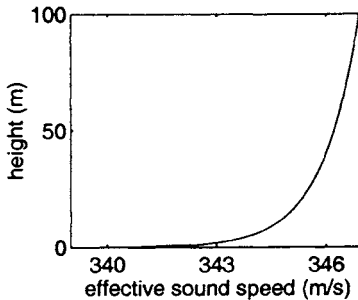


Figure 4.3. Logarithmic profile (4.5) of the effective sound speed, for $c_0 = 340 \text{ m/s}$, $z_0 = 0.1 \text{ m}$, and $b = 1 \text{ m/s}$.

atmosphere with a constant temperature, the values $b = 1 \text{ m/s}$ and $z_0 = 0.1 \text{ m}$ correspond to a wind speed (component) of 4.6 m/s at a height of 10 m .

4.4 Ray model

Atmospheric sound propagation can be modeled with sound rays. Basically, the approach of a ray model consists of two steps:

- i) calculation of the paths of all sound rays between the source and the receiver,
- ii) calculation of the received sound pressure by summation of the contributions of all sound rays.

This approach is called geometrical acoustics. The principles of geometrical acoustics are described in Refs. [2, 17, 106].

The model described in Chap. 3 for sound propagation in a non-refracting atmosphere can be considered as a simple ray model. The complex pressure amplitude p_c was written in Eq. (3.2) as a sum of two terms:

$$p_c = \sum_{m=1}^2 A_m \exp(i\phi_m), \quad (4.6)$$

with phases $\phi_m = kR_m$ and amplitudes A_m that follow by comparison with Eq. (3.2). In general, A_2 is complex, so ϕ_2 is not the total phase of the second term. The two terms can be interpreted as the contributions of sound rays. The first term represents the direct ray and the second term represents the ray reflected by the ground surface. In this case the ray model can be considered as a representation of the exact solution of the wave equation for a system with a non-refracting atmosphere and a finite-impedance ground surface (see Sec. D.4).

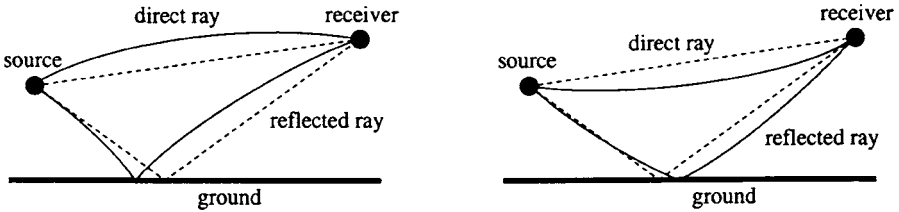


Figure 4.4. Direct ray and ray reflected by the ground surface, in a downward refracting atmosphere (left) and an upward refracting atmosphere (right). The dashed lines represented the straight rays in a non-refracting atmosphere.

In general, the assumption of a non-refracting atmosphere is justified only for small propagation distances, of the order of a few tens of meters. For larger distances, the effects of atmospheric refraction must be taken into account. In a refracting atmosphere, sound rays are curved and the number of rays is often different from two.

For small source-receiver distances, the number of rays is still equal to two, but the rays are curved as shown in Fig. 4.4. A solution of the wave equation for this situation, analogous to the exact solution for a non-refracting atmosphere, can be found in Ref. [82].

For larger distances, the number of rays is often different from two. This is illustrated in Figs. 4.5 and 4.6, for an upward refracting atmosphere and a downward refracting atmosphere, respectively. The figures show sound rays emitted by a point source within a limited interval of the elevation angle (a point source emits sound rays in all directions, but for graphical clarity we have omitted rays with large elevation angles in the figures). The rays were calculated for the logarithmic sound speed profile (4.5), with $b = -1 \text{ m/s}$ for Fig. 4.5 and $b = 1 \text{ m/s}$ for Fig. 4.6.

In an upward refracting atmosphere (Fig. 4.5), a region exists where no sound rays arrive. This region is called the shadow region. The location of the shadow region depends on the source height and the sound speed profile. The ray model predicts a vanishing sound pressure in a shadow region. In reality, the sound pressure is small but not zero, due to the effect of diffraction and the effect of scattering by atmospheric turbulence [89] (see Sec. 4.6.4 and Chap. 5).

In a downward refracting atmosphere (Fig. 4.6), sound rays with multiple ground reflections occur, so the number of rays arriving at a distant receiver is often much larger than two. The calculation of all ray paths to a receiver is called ‘ray tracing’. One needs in general an iterative computational algorithm to ‘trace’ all ray paths. A ray tracing algorithm consists basically of the computation of many ray paths and the selection of those ray paths that arrive at the receiver. A ray path is computed by numerical integration of Snell’s law (4.3), *i.e.* by making small steps along the ray path in such a way that the elevation angle satisfies Snell’s law (4.3) at all points of the ray path. Figure 4.7 shows that the number of rays increases with increasing distance between the source

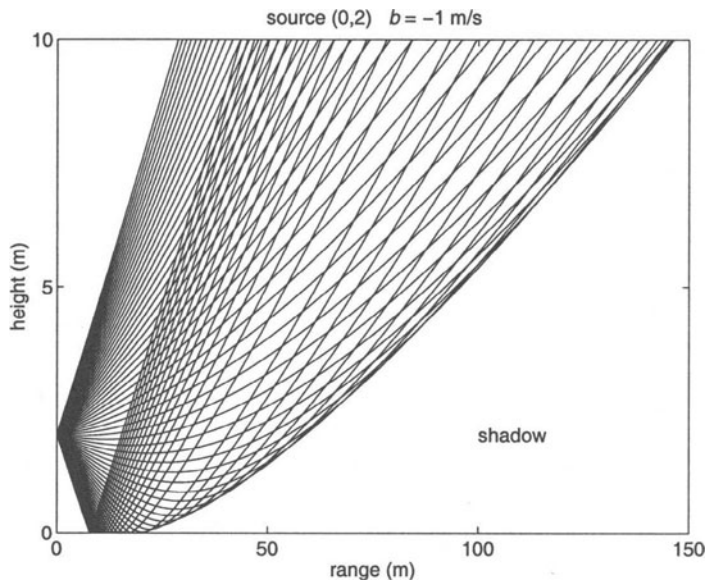


Figure 4.5. Sound rays in an upward refracting atmosphere.

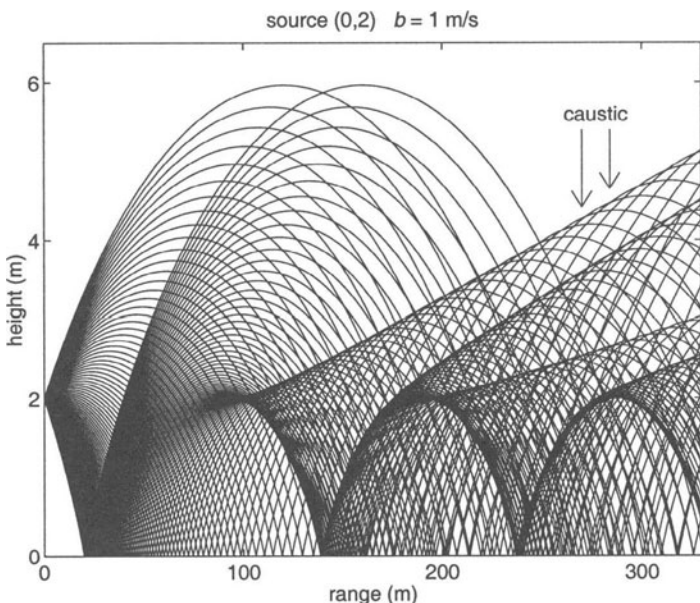


Figure 4.6. Sound rays in a downward refracting atmosphere.

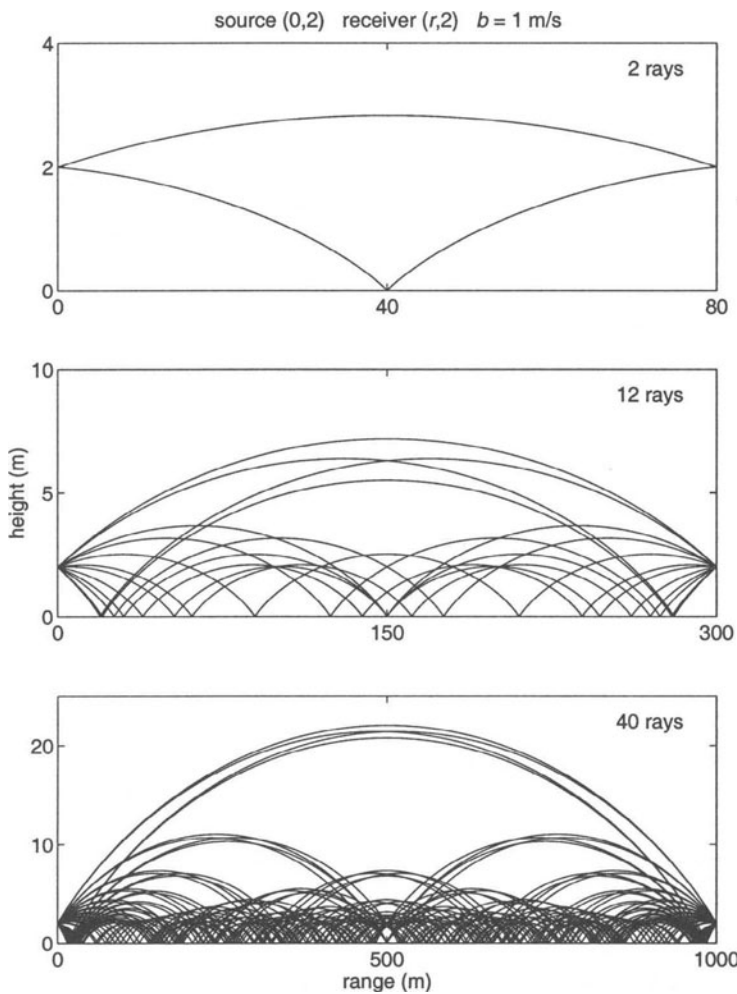


Figure 4.7. Sound rays between a source at position $(0,2)$ and a receiver at position $(r,2)$, for $r = 80$ m (top), $r = 300$ m (middle), and $r = 1000$ m (bottom), in a downward refracting atmosphere with logarithmic sound speed profile (4.5) with $b = 1$ m/s. The lower graph for $r = 1000$ m illustrates the grouping of rays in sets of four rays.



Figure 4.8. The ray tube diameter D is the normal distance between two sound rays emitted by the source with a small difference in elevation angle.

and the receiver, for a logarithmic sound speed profile. The figure also shows that the rays are grouped in sets of four rays [49], except for small distances between the source and the receiver.

The generalization of Eq. (4.6) for a situation with two or more sound rays in a downward refracting atmosphere is [17, 81, 135]

$$p_c = \sum_{m=1}^{N_{\text{rays}}} A_m \exp(i\phi_m), \quad (4.7)$$

where N_{rays} is the number of sound rays. The phase ϕ_m of ray m is given by $\phi_m = \int k(z)ds$, where s is the path length along the ray; we assume a layered atmosphere here, with $k = k(z)$. This can also be written as $\phi_m = \omega t_m$, where $t_m = \int c^{-1}(z)ds$ is the travel time along the ray. The amplitude A_m of ray m can be written as (see Sec. L.3)

$$A_m = f_m C_m^{N_m} \frac{S}{R_1}, \quad (4.8)$$

where f_m is a focusing factor, C_m is a reflection coefficient, and N_m is the number of ground reflections. For the reflection coefficient C_m we use the spherical-wave reflection coefficient (see Sec. L.3.4). The focusing factor f_m accounts for the fact that, in a refracting atmosphere with curved sound rays, there are regions where the ‘concentration’ of sound rays is high and regions where the ‘concentration’ of sound rays is low (see Fig. 4.6). A measure of the ray concentration is the ray tube diameter D , which is defined as the normal distance between two sound rays emitted by the source with a small difference in elevation angle (see Fig. 4.8). The ray tube diameter is small in regions of high ray concentration (the rays are focused here) and the ray tube diameter is large in regions of low ray concentration (the rays are defocused here). The focusing factor is equal to $\sqrt{D_{\text{free}}/D}$, where D_{free} is the ray tube diameter in the free field, *i.e.* the field in an unbounded homogeneous atmosphere (see Sec. L.3.6). The focusing factor is equal to unity in the free field.

A problem with the ray model is caustics [18, 17, 106]. A caustic is a set of points where the ray tube diameter vanishes. In other words, two sound rays emitted by the source with a small (infinitesimal) difference in elevation angle, cross each other at a caustic point (see Fig. 4.6). Hence, the focusing factor diverges at a caustic point, and geometrical acoustics predicts an infinite

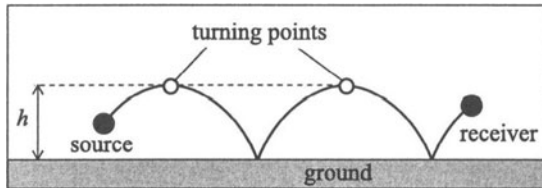


Figure 4.9. Example of a sound ray with two turning points ($n = 2$). The maximum height of the ray, denoted as h , is indicated.

amplitude at a caustic point. In reality, the amplitude of the sound pressure at a caustic point is relatively high but not infinite of course. The difference between the real sound pressure field and the geometrical acoustics prediction is called a caustic diffraction field. Caustic diffraction fields eliminate the infinite amplitudes. The computation of caustic diffraction fields is complex [85, 73], which makes the ray model less attractive for accurate computations of sound propagation, in particular for irregular sound speed profiles.

In Appendix L we describe a ray model that takes into account caustic diffraction fields. The model assumes a smooth sound speed profile, with a sound speed that increases monotonically with height; an example is the logarithmic profile (4.5). The rays shown in Figs. 4.6 and 4.7 for a downward refracting atmosphere were computed with this model (the rays shown in Fig. 4.5 for an upward refracting atmosphere were computed by straightforward integration of Snell's law).

In the remainder of this section we will use the ray model to provide insight into sound propagation in situations such as shown in the lower graph in Fig. 4.7 (for $r = 1000$ m), with a large distance between the source and the receiver and a large number of sound rays. The sound rays are grouped in sets of four rays. In the example shown in the lower graph in Fig. 4.7, there is a group of four rays that reach a height of about 22 m, a second group of four rays that reach a height of about 11 m, and so on. In general, the highest point of a sound ray is called the turning point, and the height of the turning point is called the maximum height of the ray; the maximum height is denoted as h (see Fig. 4.9). The four rays of a group have an equal number of turning points, which is denoted as n ($n = 1, 2, \dots$). The maximum height h is approximately equal for the four rays of a group, and we denote the value of h for a group of rays with n turning points as h_n . For the logarithmic profile (4.5) we have (see Sec. L.3.1)

$$h_n \approx \frac{r}{n} \sqrt{\frac{b}{2\pi c_0}}. \quad (4.9)$$

For $r = 1000$ m and $b = 1$ m/s we find $h_n \approx 22/n$ m. Thus, we have $h_1 \approx 22$ m, $h_2 \approx 11$ m, and so on. These values are in agreement with the maximum heights of the rays shown in the lower graph in Fig. 4.7.

Equation (4.9) for the maximum height h_n is valid if the source height z_s and the receiver height z are small compared with h_n . With increasing n , the maximum height h_n decreases and deviations occur from Eq. (4.9). At a certain value of n , h_n given by Eq. (4.9) becomes smaller than z_s or z , and Eq. (4.9) should not be used anymore, as there are no sound rays with a maximum height smaller than z_s or z .

If we neglect the deviations from Eq. (4.9) and use this equation for all rays with h_n larger than z_s and z , we find that the total number of groups is given approximately by h_1/z_{sr} , where z_{sr} is, for example, the average of the source height and the receiver height. Each group consists of four rays, so the total number of rays is $N_{\text{rays}} \approx 4h_1/z_{sr}$. In the example in the lower graph in Fig. 4.7, $4h_1/z_{sr}$ is equal to 44, in good agreement with the actual number of rays (40).

The relation $N_{\text{rays}} \approx 4h_1/z_{sr}$ can be used to derive a simple expression for the relative sound pressure level ΔL for the case of sound propagation over a water surface in a downward refracting atmosphere with logarithmic sound speed profile (4.5). As the reflection coefficient for a water surface is equal to unity, all rays have approximately equal amplitudes at a distant receiver; here we neglect the effects of focusing and caustics. We further neglect the effects of interference between the rays, so we assume that the phases of the rays are random. In the free field there is only one ray, so we have $|p_c|^2 \approx N_{\text{rays}}|p_{\text{free}}|^2$ in the definition (3.6) of ΔL . This gives

$$\Delta L \approx 10 \lg N_{\text{rays}}, \quad (4.10)$$

where $N_{\text{rays}} = 4h_1/z_{sr}$ is the number of rays. It follows from Eq. (4.9) that N_{rays} is proportional to the receiver range r , so it follows from Eq. (4.10) that ΔL increases linearly with $\lg r$. In Sec. 4.6.4 we will illustrate this linear increase by a numerical example. In Chap. 6 we will see that the increase is not unlimited, as a consequence of the roughness of a water surface.

In the case of sound propagation over an absorbing ground surface, *e.g.* grassland, the above linear increase of ΔL with $\lg r$ does not occur. In this case, rays with many ground reflections have a small amplitude at a distant receiver. Consequently, most of the sound energy flows along the highest sound rays [131]. In this case the relative sound pressure level ΔL at a distant receiver is dominated by the highest sound rays.

4.5 FFP and PE methods

In this section we describe three accurate numerical methods for sound propagation in a refracting atmosphere over a ground surface:

- the Fast Field Program (FFP),
- the Crank-Nicholson Parabolic Equation (CNPE) method,
- the Green's Function Parabolic Equation (GFPE) method.